Available online at www.sciencedirect.com
SCIENCE DIRECT®
Applied Surface Science 252 (2006) 5839–5845
applied surface science
www.elsevier.com/locate/apsusc

Oxidation of Zircaloy-4 by H_2O followed by molecular desorption

N. Stojilovic, R.D. Ramsier *

Departments of Physics and Chemistry, The University of Akron, Akron, OH 44325-4001, USA

Received 11 May 2005; accepted 1 August 2005
Available online 8 September 2005

Abstract

The interaction of H_2O with Zircaloy-4 (Zry-4) is investigated using Auger electron spectroscopy (AES) and temperature programmed desorption (TPD) methods. Following adsorption of H_2O at 150 K the Zr(MNV) and Zr(MNN) Auger features shift by ~6.5 and 4.5 eV, respectively, indicating surface oxidation. Heating H_2O/Zry-4 results in molecular desorption of water at both low and high temperatures. The low-temperature desorption is attributed to ice multilayers, whereas, three overlapping high-temperature features are presumably due to recombinative desorption. This high-temperature desorption begins before the surface oxide is dissolved, continues upon its removal, and is atypical for water/metal systems. Unexpectedly, no significant desorption of hydrogen is observed near 400 K, as is typically observed following O_2 adsorption on Zr-based materials. However, we do observe that H_2O adsorption on Zry-4 surfaces roughened by argon ion sputtering results in H_2 desorption.

Keywords: Zircaloy-4; Water; TPD; AES; Zero-order desorption kinetics

1. Introduction

Understanding and controlling the interaction of water with solid surfaces is relevant from both technological and fundamental points of view. Consequently, the number of articles dealing with the behavior of water on solid surfaces is overwhelming; see for example review articles by Thiel and Madey [1], and later by Henderson [2]. Despite the fact that much research has been published on the subject, little is known about the surface chemistry of water on zirconium-based materials. Since Zircaloy-4 (Zry-4) serves as a structural material exposed to hot water in nuclear reactors, understanding the oxidation of Zry-4 by water is of applied interest. In addition, the unique mass-transport processes previously observed on Zr surfaces are fundamentally important as well [3,4], and it is relevant to investigate whether similar behavior is observed for Zr alloys.

A previous photoelectron study of polycrystalline zirconium revealed that at 100 K water mainly

* Corresponding author.
E-mail address: rex@uakron.edu (R.D. Ramsier).

0169-4332/$ – see front matter
doi:10.1016/j.apsusc.2005.08.006

dissociates into H_{ads} and O_{ads}, with small amounts of OH_{ads} detected [5]. In a study of D_2O adsorption on Zr(0 0 0 1) at low temperatures similar dissociation products were observed, and no low-temperature oxide formation or water desorption was reported for low coverages [6]. It is interesting that in this study no hydrogen desorption was reported during water adsorption at 80 or 158 K [6], whereas, in a follow-up study molecular hydrogen desorption was observed during water adsorption above 170 K [7]. On the other hand, an investigation of D_2O/Zr(0 0 0 1) performed in our laboratory by backfilling methods at 160 K revealed high-temperature desorption of water but no surface oxidation prior to electron bombardment [8]. Desorption of water in one case [8] and lack of desorption in the other [6] might be explained by differences in coverage and adsorption temperatures. In the present study of H_2O adsorption on Zry-4 at 150 K, we employ relatively high H_2O exposures using a molecular beam doser [9], specifically to investigate surface oxide formation and desorption kinetics.

Because zirconium and its alloys are in essence gettering materials, especially for oxygen, understanding the chemistry of these surfaces is difficult. Our motivation to study the H_2O/Zry-4 system at low temperatures is to connect the chemistry observed on this alloy, containing more than 98% zirconium, to results obtained on zirconium single crystals [6–8]. We ultimately aim to understand both oxidation and desorption kinetics on these reactive surfaces. In this article, using Auger electron spectroscopy (AES) and temperature programmed desorption (TPD) methods we investigate the interaction of H_2O with Zry-4. We observe surface oxidation by H_2O adsorption at 150 K, and report high-temperature water desorption that exhibits some characteristics of zero-order kinetics. Additionally, we do not observe significant hydrogen desorption as previously detected after water adsorption on Zr(0 0 0 1) [6,8], and oxygen adsorption on other Zr surfaces [10–12].

2. Experimental

The Zry-4 sample used in this study had a thickness of 2 mm and surface area of 0.53 cm^2. The elemental composition of Zry-4 in wt.% is nominally 1.2% Sn, 0.2% Fe, 0.2% Cr + O + Si, and the balance Zr. The surface was cleaned by sputtering and short annealing at ~920 K to dissolve traces of carbon and oxygen as confirmed using AES. Under these conditions the Sn(MNN)/Zr(MNN) ratio was below 0.12, as we reported recently [13]. The AES signatures of other alloying elements are at the edge of detection limits. Deionized water used in this study was further purified by several freeze-pump-thaw cycles and the cleanliness of the vapor was verified using a quadrupole mass spectrometer (QMS). The gas-handling system was pumped by a turbo-molecular pump prior to each experiment. For TPD experiments the sample was facing the QMS in a line-of-sight geometry, and the sample temperature was increased at the rate of 1.8 K/s by resistive heating. Experiments were performed at base pressures of approximately 3.0×10^{-10} Torr. More details about our ultra-high vacuum chamber are given elsewhere [14,15].

3. Results and discussion

Fig. 1 shows Auger electron spectra of a Zry-4 surface after cleaning, and following a series of exposures to H_2O at approximately 150 K. Here we focus on how the zirconium Auger features change as a function of water exposure. Note that exposures of $10.2 \times 10^{14}/cm^2$ are sufficient to significantly reduce the Zr(MNV) and Zr(MNN) peak intensities, shift their positions, and change the shape of the Zr(MNV) feature. Vertical lines are inserted to indicate shifts in Auger peak positions. The change in peak intensities most likely originates from shielding effects. Shifts in peak positions toward lower kinetics energies indicate oxidation of the surface whereas changes in the shape of the Zr(MNV) features result from the transfer of valence electrons from the metal to oxygen [16]. Note that for higher H_2O exposures shifts of 6.5 eV for the Zr(MNV) and 4.5 eV for the Zr(MNN) features (±0.5 eV), are observed. A shift in the Zr(MNV) feature of 7 eV corresponds to a change in oxidation state of zirconium from 0 to +4 [17]. Also note that for exposures above $82.0 \times 10^{14}/cm^2$ no significant shifts in peak positions or changes in feature profiles are observed. At this point the near-surface region saturates with oxygen.

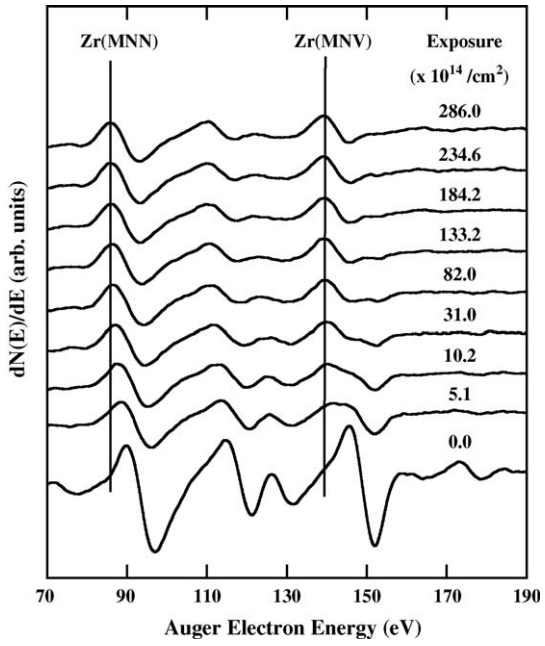

Fig. 1. Zirconium Auger features for various water exposures. Exposures, given in units of 10^{14}/cm^2 are: 0.0, 5.1, 10.2, 31.0, 82.0, 133.2, 184.2, 234.6, and 286.0. Spectra are shifted vertically for clarity while vertical lines are inserted to indicate shifts in peak positions. The Zr(MNV) and Zr(MNN) features shift by 6.5 and 4.5 eV, respectively, revealing surface oxidation by H_2O adsorption at 150 K.

It is worth mentioning that unlike oxygen [10], water adsorption at 150 K notably changes the intensity of the Zr(MNN) feature. In a related study, Auger electron spectra of zirconium exposed to O_2 and H_2O reveal that the intensity of the Zr(MNN) feature is reduced more upon exposure to H_2O [18]. In the same study it was speculated that the presence of hydrogen from dissociated water molecules had an effect on Auger signal intensities. Our results imply that hydrogen stays in the near-surface region of Zry-4 after water adsorption at 150 K, consistent with Ref. [6], and also that the presence of hydrogen may have an effect on the Zr(MNN) transition, consistent with Ref. [18]. It is not surprising that these present results for H_2O/Zry-4 using high fluxes and exposures (with a molecular beam doser) differ from those observed for low water exposures at low fluxes (using backfilling) reported previously for D_2O/Zr(0 0 0 1) [8] from our laboratory. No oxidation of the surface of Zr(0 0 0 1) was observed in this previous case, and electron bombardment effects resulted in a shift of the Zr(MNV) feature by 2 eV.

Fig. 2 shows how zirconium (A) and oxygen (B) Auger features change when Zry-4 is exposed to water (200.0×10^{14}/cm^2) and then stepwise annealed. The uppermost spectral lines in both panels represent the

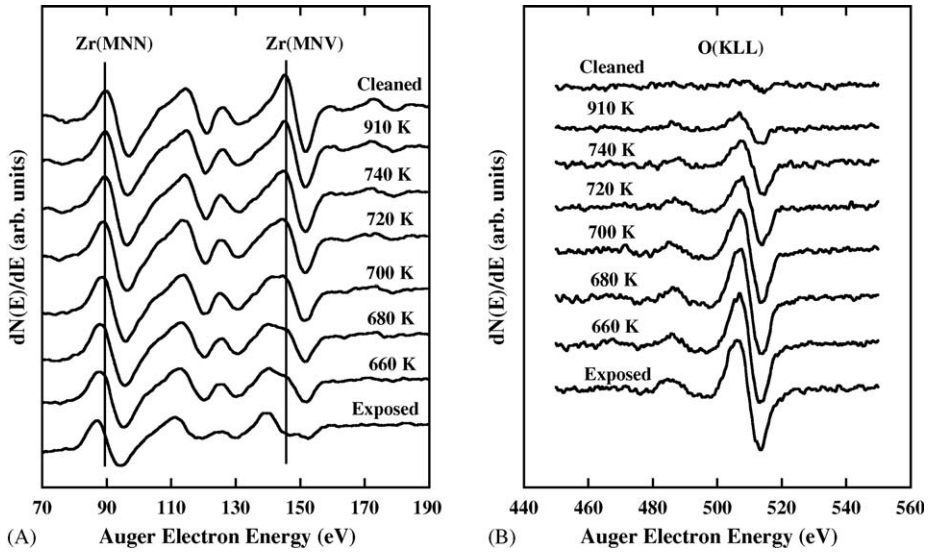

Fig. 2. Zirconium (A) and oxygen (B) Auger features after H_2O exposure (200.0×10^{14}/cm^2) at 150 K, and after stepwise annealing. The oxide layer is removed near 700 K as can be inferred from the shift of the Zr(MNV) and Zr(MNN) features back to their initial clean surface positions. Note that annealing up to 910 K leaves some oxygen in the near-surface region (panel B).

surface after sputtering and annealing, prior to gas adsorption experiments. When the exposed surface is annealed to 660 K the Zr(MNV) feature changes shape. At this temperature, as will be shown later, significant desorption of water takes place. Note that at 700 K or above the Zr(MNV) and Zr(MNN) features shift back to their initial clean surface values, indicating removal of the surface oxide, with a significant amount of oxygen left in the near-surface region. Panel B shows how the O(KLL) Auger peak changes intensity without shifting significantly. Annealing to 910 K leaves some oxygen in the near surface region that can be removed by one sputtering/annealing cycle. The uppermost spectrum of panel B also shows that in our experiments, before gas-adsorption experiments, the oxygen content in the near-surface region is reduced to the detection limit of our AES system. Although not shown here, the carbon content of the near-surface region is also negligible.

To a good approximation, the TPD spectra of Fig. 3 show low-temperature desorption of water with a common leading edge and upward shift in peak maxima with exposure, characteristic of zero-order desorption kinetics [19]. Note that for exposures below $25.0 \times 10^{14}/\text{cm}^2$ no significant molecular desorption is observed. However, at these low exposures, the Zr(MNV) and Zr(MNN) features are strongly perturbed (Fig. 1). We propose that the first adsorbed layer(s) mostly dissociate on the surface during adsorption at 150 K, preventing the formation of an ice layer. For higher exposures the desorption of water multilayers is observed. Calculating the area below the features, we find that the yield increases with exposure and shows no signs of saturation up to $566.1 \times 10^{14}/\text{cm}^2$. Using leading edge TPD analysis [20] for zero-order desorption kinetics, from Arrhenius plots of ln(Intensity) versus $1/T$, we estimate the activation energy of desorption to be 53 kJ/mol. Desorption of these multilayers occurs from an oxidized surface, as our AES data clearly indicate.

Fig. 4 shows high-temperature desorption of water with three overlapping desorption peaks, α, β, and γ, observed at higher exposures. Note that all three features shift toward higher temperatures, with the γ

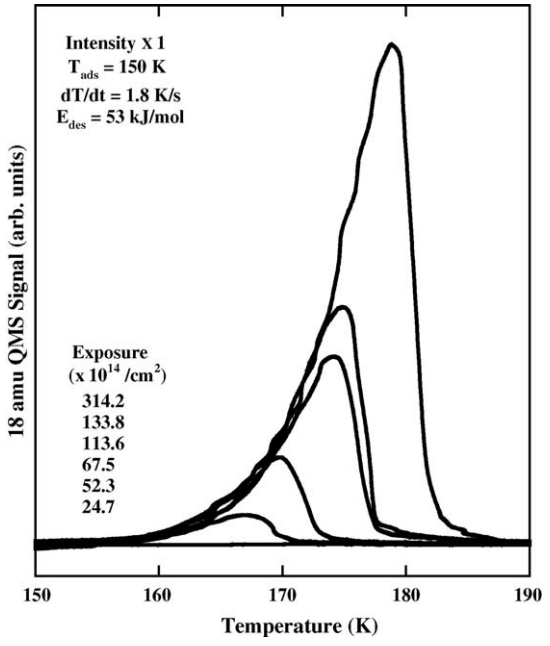

Fig. 3. Low-temperature desorption of water following H_2O adsorption on Zry-4 at 150 K, revealing zero-order desorption kinetics with an estimated activation energy for desorption of 53 kJ/mol. Exposures, given in units of $10^{14}/\text{cm}^2$ are: 24.7, 52.3, 63.5, 113.6, 133.8, and 314.25. The heating rate was 1.8 K/s.

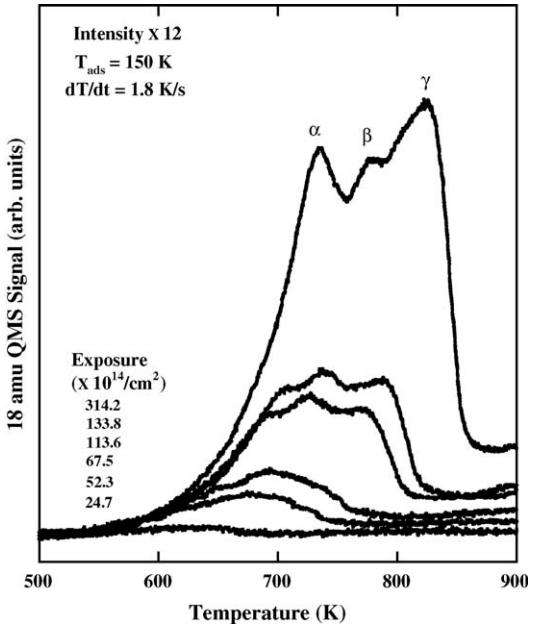

Fig. 4. High-temperature desorption of water following H_2O adsorption on Zry-4 at 150 K, with behavior that resembles zero-order desorption kinetics. Exposures and heating rates are identical to those in Fig. 4.

peak shifting above 800 K and becoming dominant at the highest exposures. TPD yields of these high-temperature desorption features, calculated as the area below all three features, also increase with exposure, similar to those of ice multilayers. Initially, at low exposures, water mostly dissociates, consistent with results obtained on Zr(0 0 0 1) surfaces [6,8]. Even though Fig. 4 shows no obvious TPD features after the lowest exposure (24.7×10^{14}/cm^2), on a more-sensitive scale, we observe one small peak with poor signal-to-noise ratio, near 630 K. These complicated desorption kinetics occurring at high temperatures are not typical for water–metal interactions [1].

Our interpretation of these results is as follows. At low exposures, H_2O dissociates and subsequent heating dissolves the oxygen into the bulk. At higher exposures, since much more water desorbs from the surface as compared to the case when oxygen is adsorbed [10], we propose that some of the hydrogen resides in the near-surface region. Water desorption is significant when the near-surface region of Zry-4 saturates with oxygen. Heating of H_2O/Zry-4 in this case results in recombinative desorption of H_2O at high temperature and ice desorption at low temperature with kinetics that resemble that of zero order.

In order to further investigate similarities with zero-order desorption kinetics we performed isothermal desorption experiments. Fig. 5 presents isothermal (750 K) desorption spectra of water obtained after

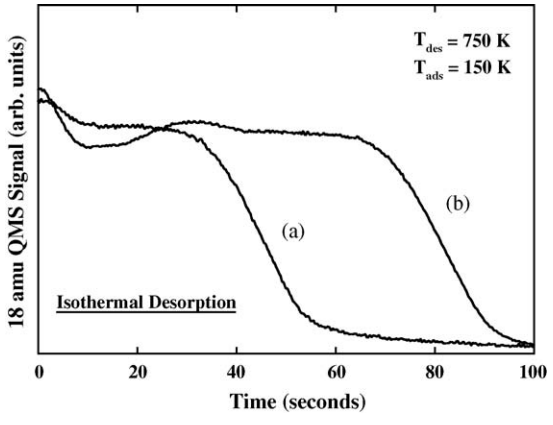

Fig. 5. Isothermal desorption spectra of water taken at 750 K after H_2O adsorption of (a) 314.2×10^{14}/cm^2 and (b) 566.1×10^{14}/cm^2 near 150 K. Nearly flat regions in isothermal desorption spectra usually indicate zero-order desorption kinetics.

H_2O exposures of (a) 314.2×10^{14}/cm^2 and (b) 566.1×10^{14}/cm^2 at 150 K. Nearly flat regions are characteristic of zero-order desorption [21]. Note that for higher exposures the time interval for the nearly flat region is longer. This is consistent with the fact that for our exposures studied here no saturation in TPD yield is observed. The exact mechanism behind this recombinative desorption is not clear at present. The fact that desorption starts near 550 K, whereas, the surface oxide is removed near 700 K makes the interpretation even more difficult.

In a study of the interaction of water with (2×1) surfaces of α-Fe_2O_3(0 1 2), recombinative desorption close to 400 K with pseudo-zero order kinetics was reported [22]. Unlike the study of water on α-Fe_2O_3(0 1 2), we observe recombinative desorption of H_2O from Zry-4 with three desorption peaks at much higher temperatures, where the γ peak is above 800 K for higher exposures. Since our results indicate complicated desorption profiles of water with some characteristics of zero order desorption they are interesting from a fundamental point of view. Our preliminary results from D_2O/Zr(0 0 0 1) using a molecular beam doser (not shown) also revealed three desorption states at similar desorption temperatures, minimizing the possible role of Zry-4 alloying elements in the formation of these three desorption peaks.

Note that three peaks are observed using a molecular beam doser in this study, whereas, only one peak near 700 K was observed in backfilling experiments [8]. This type of difference was also observed for C_6H_6/Zr(0 0 0 1) using backfilling [4] and later molecular beam doser [23] methods, and is possibly due to partial desorption from the sample holder assembly and reduced pumping speed in our previous backfilling experiments. Here, we also propose that the difference in flux rates may play a role in these apparent discrepancies. To support this position, we exposed Zry-4 to $\sim$10 L of H_2O by backfilling the vacuum system and observed only one desorption peak (not shown), consistent with what was observed on Zr(0 0 0 1) [8]. Since dissolution of oxygen into the subsurface region is involved, high fluxes (doser) of water may be expected to behave differently than low fluxes (backfilling), and may be similar to previous observations concerning the pressure dependence of oxygen adsorption on Zr surfaces [24]. Relatively broad TPD features and very

high desorption temperatures are not surprising when one considers that zirconium is a gettering material for common gases. For example, the solid solubility of oxygen in α-Zr(O) is approximately 30 at.% [25].

Another interesting result of this present study is the absence of significant hydrogen desorption near 400 K. Several studies of zirconium-based materials have reported molecular hydrogen desorption in the 400–500 K range that is attributed to the presence of oxygen [10–12]. In our recent study of the $^{18}O_2$/Zry-4 system [10], this H_2 desorption is observed following $^{18}O_2$ adsorption at both 150 and 300 K. Interestingly, for H_2O/Zry-4, even though a significant amount of hydrogen is expected to reside in the near-surface region, the desorption of H_2 is at or below the detection limit. Besides rapid desorption of bulk hydrogen [12,23] above 800 K, our TPD experiments show no significant H_2 desorption from sputter-cleaned and annealed Zry-4 surfaces.

However, Fig. 6 shows effects of surface roughening on hydrogen desorption following low (A) and high (B) exposure of Zry-4 to H_2O near 150 K. In both panels the upper spectra show desorption from surfaces that were sputtered and not annealed, whereas, the lower spectra are from surfaces that were sputtered and annealed prior to water adsorption. Note that regardless of exposure there is hydrogen desorption from water adsorbed on the sputtered surfaces. Previously we observed that 1 h of bombardment by 2 keV argon ions is sufficient to destroy the surface structure of Zr(0 0 0 1), as inferred from low-energy electron diffraction (not shown).

Here, in the case of Zry-4, we propose that sputtering produces surface defects that promote hydrogen desorption, which are not present when the sample is annealed. The role of argon embedded in the near-surface region after sputtering (Ar(LMM)/Zr(MNN) $\sim$ 0.06) cannot be ruled out; neither can the possible increase in exposed surface area due to roughening. However, we observe that from sputtered surfaces exposed to H_2O without annealing, increases in water exposure result in larger quantities of desorbing hydrogen. It is possible that the defect sites produced by sputtering (without annealing) decompose more water than annealed surfaces, or open channels for more rapid oxygen diffusion into the subsurface. Both mechanisms could account for an increase in surface-stabilized H that combines during heating to desorb at H_2.

The fact that we do not observe hydrogen desorption following exposure of annealed Zry-4 to H_2O is puzzling, especially when we know that adsorption of O_2 on zirconium [11,12] and D_2O on Zr(0 0 0 1) [6,8] results in hydrogen desorption in the 300–500 K range. In one study, zirconium was exposed to oxygen and then to D_2 to rule out the possibility that the origin of the hydrogen TPD peak was background contamination during oxygen

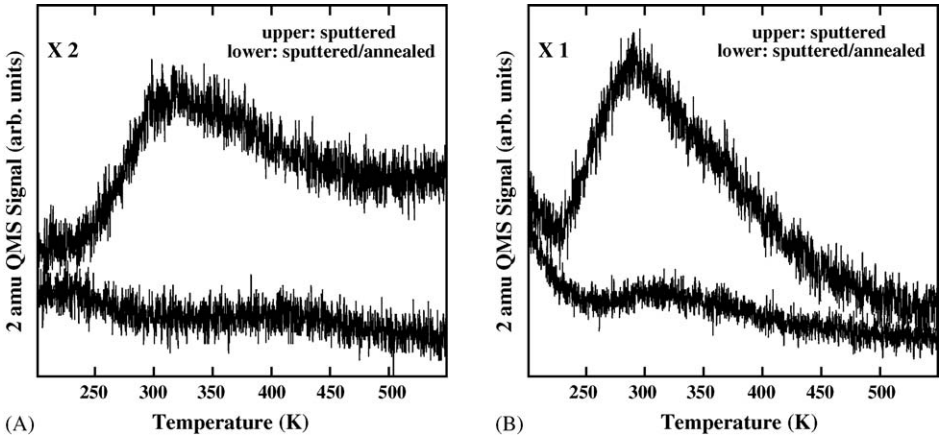

Fig. 6. TPD spectra of H_2 after adsorption of water on Zry-4 surfaces at (A) low exposure (1.7×10^{14}/cm^2), and (B) high exposure (300.0×10^{14}/cm^2). Each panel shows data from sputtered (upper spectra) and sputtered/annealed surfaces (lower spectra). The adsorption temperature was approximately 150 K and the heating rate was 1.8 K/s.

adsorption [12]. In a study on Zr(0 0 0 1) [6], it was proposed that the hydrogen observed in TPD originates from dissociated water, whereas, in a study on polycrystalline zirconium [12], it was observed that hydrogen was attracted to the surface from the bulk by adsorbed oxygen. If these interpretations are correct, there are two different origins of the same desorbing species. This indicates the complex nature of the surface chemistry of Zr-based materials.

4. Summary

For higher exposures of Zry-4 to H_2O near 150 K, we observe molecular desorption both at low and high temperatures. Desorption below 200 K is from ice multilayers, whereas, high-temperature features correspond to recombinative desorption. Three desorption peaks at unexpectedly high temperatures all shift toward higher temperatures with exposure and exhibit unique desorption profiles. For low exposures, the Zr(MNN) Auger feature that is typically not significantly perturbed by the presence of oxygen is reduced in intensity following low-temperature H_2O adsorption. For higher exposures, the Zr(MNV) and Zr(MNN) Auger features shift by $\sim$6.5 and 4.5 eV, respectively, indicating surface oxidation. The surface oxide is removed near 700 K during heating whereas water desorption starts near 550 K, making the interpretation of high-temperature desorption kinetics complicated. Some similarities with zero-order desorption kinetics, however, are evident.

References

[1] P.A. Thiel, T.E. Madey, Surf. Sci. Rep. 7 (1987) 211.
[2] M.A. Henderson, Surf. Sci. Rep. 46 (2002) 1.
[3] Y.C. Kang, R.D. Ramsier, Surf. Sci. 519 (2002) 229.
[4] N. Stojilovic, R.D. Ramsier, Solid State Commun. 130 (2004) 623.
[5] R. Zehringer, R. Hauert, P. Oelhafen, H.-J. Guntherodt, Surf. Sci. 215 (1989) 501.
[6] B. Li, K. Griffiths, C.-S. Zhang, P.R. Norton, Surf. Sci. 370 (1997) 97.
[7] B. Li, K. Griffiths, C.-S. Zhang, P.R. Norton, Surf. Sci. 384 (1997) 70.
[8] S. Ankrah, Y.C. Kang, R.D. Ramsier, J. Phys.: Condens. Mat. 15 (2003) 1899.
[9] N. Stojilovic, J.C. Tokash, R.D. Ramsier, Surf. Sci. 565 (2004) 243.
[10] N. Stojilovic, E.T. Bender, R.D. Ramsier, submitted for publication.
[11] W.J. Peterson, R.E. Gilbert, G.B. Hoflund, Appl. Surf. Sci. 24 (1985) 121.
[12] D.A. Asbury, G.B. Hoflund, W.J. Peterson, R.E. Gilbert, R.A. Outlaw, Surf. Sci. 185 (1987) 213.
[13] N. Stojilovic, E.T. Bender, R.D. Ramsier, Appl. Surf. Sci. 252 (2005) 1806–1811.
[14] Y.C. Kang, M.M. Milovancev, D.A. Clauss, M.A. Lange, R.D. Ramsier, J. Nucl. Mater. 281 (2000) 57.
[15] Y.C. Kang, R.D. Ramsier, J. Nucl. Mater. 303 (2002) 125.
[16] T.W. Haas, J.T. Grant, G.J. Dooley, J. Appl. Phys. 43 (1972) 1853.
[17] C.-S. Zhang, B.J. Flinn, P.R. Norton, Surf. Sci. 264 (1992) 1.
[18] Y. Nishino, A.R. Krauss, Y. Lin, D.M. Gruen, J. Nucl. Mater. 228 (1996) 346.
[19] G.A. Attard, C.J. Barnes, Surfaces, Oxford University Press, Oxford, U.K., 1998 (Ch. 2.7).
[20] C.N. Chittenden, E.D. Pylant, A.L. Schwaner, J.M. White, in: A.T. Hubbard (Ed.), The Handbook of Surface Imaging and Visualization, CRC Press, Boca Raton, 1995 , pp. 817–845 (Ch. 59).
[21] K. Nagai, A. Hirashima, Surf. Sci. 187 (1987) 616.
[22] M.A. Henderson, S.A. Joyce, J.R. Rustad, Surf. Sci. 417 (1998) 66.
[23] N. Stojilovic, R.D. Ramsier, Chem. Phys. Lett. 399 (2004) 53.
[24] (a) M. Yamamoto, S. Naito, M. Mabuchi, T. Hashino, J. Chem. Soc. Faraday Trans. 87 (1991) 1591;
(b) K. Griffiths, J. Vac. Sci. Technol. A 6 (1988) 210.
[25] T. Tanabe, M. Tomita, Surf. Sci. 222 (1989) 84.